

# Appearance and disappearance signals at a $\beta$ -Beam and a Super-Beam facility

A. Donini, E. Fernández-Martínez and S. Rigolin

I.F.T. and Dep. Física Teórica, U.A.M., E-28049, Madrid, Spain

## Abstract

In this letter we present the study of the eightfold degeneracy in the  $(\theta_{13}, \delta)$  measurement including both appearance and disappearance channels. We analyse, for definiteness, the case of a standard low- $\gamma$   $\beta$ -Beam and a 4 MWatt SPL Super-Beam facility, both aiming at a UNO-like Mton water Čerenkov detector located at the Fréjus laboratory,  $L = 130$  km. In the  $\beta$ -Beam case, the  $\nu_e$  disappearance channel does not improve the  $(\theta_{13}, \delta)$  measurement when a realistic (i.e.  $\geq 2\%$ ) systematic error is included. In the Super-Beam case, the  $\nu_\mu$  disappearance channel could, instead, be quite useful in reducing the impact of the eightfold degeneracy in the  $(\theta_{13}, \delta)$  measurement, especially once the error on the atmospheric mass difference is fully taken into account in the fit.

# 1 Introduction

After more than 30 years of successful neutrino oscillation experiments [1] two parameters still remain undetermined in the three-family Pontecorvo-Maki-Nakagawa-Sakata [2] mixing matrix: the mixing angle  $\theta_{13}$ , for which only a upper limit has been set [3], and the CP-violating phase  $\delta$  that is still completely unknown. The full understanding of the leptonic mixing matrix constitutes, together with the discrimination of the Dirac/Majorana character and the measure of the neutrino absolute mass scale, the main neutrino-physics goal for the next decade(s).

It is well known that the best way to simultaneously measure  $(\theta_{13}, \delta)$  is the (golden)  $\nu_e \rightarrow \nu_\mu$  appearance channel [4] (and its T and CP conjugate ones). Unfortunately this measure is, in general, severely affected by the presence of degeneracies. When a measurement of the two unknown parameters is performed using a beam able to produce both neutrinos and antineutrinos, the following four systems of equations must be solved:

$$\begin{cases} N_{l^+}(\bar{\theta}_{13}, \bar{\delta}; \bar{s}_{atm}, \bar{s}_{oct}) &= N_{l^+}(\theta_{13}, \bar{\delta}; \pm \bar{s}_{atm}, \pm \bar{s}_{oct}), \\ N_{l^-}(\bar{\theta}_{13}, \bar{\delta}; \bar{s}_{atm}, \bar{s}_{oct}) &= N_{l^-}(\theta_{13}, \bar{\delta}; \pm \bar{s}_{atm}, \pm \bar{s}_{oct}), \end{cases} \quad (1)$$

where  $s_{atm} = sign(\Delta m_{atm}^2)$  and  $s_{oct} = sign(\tan 2\theta_{23})$  are two discrete unknowns, the sign of the atmospheric mass difference and the  $\theta_{23}$ -octant. The r.h.s. of this equation implies that four different models (each of them with a definite  $(s_{atm}, s_{oct})$  choice) must be used to fit the data on the l.h.s. The eight solutions form what is known as the *eightfold degeneracy* [5]-[8]. Various methods have been considered to get rid of degeneracies (using spectral analysis [5], combination of experiments [9] and/or different channels [10]). In principle, the eightfold degeneracy can be completely solved if a sufficient number of independent informations is added. At the cost, of course, of increasing the number of detectors and/or beams and consequently the budget needs.

In this letter we try to understand if the effect of degeneracies can be reduced using informations from both the appearance and the disappearance channels at a single experiment. We consider as a reference the proposal for two CERN-based facilities, the standard<sup>1</sup> low- $\gamma$   $\beta$ -Beam [11] and the Super-Beam based on the 4 MWatt SPL 2.2 GeV proton driver [15]. Both beams are directed from CERN toward the underground Fréjus laboratory, where it has been proposed to locate a 1 Mton UNO-like [16] water Čerenkov detector with a 440 kton fiducial mass. The considered baseline is  $L = 130$  km. To be at the first peak in the leading oscillation probability term, the average neutrino energy for both beams has been chosen of the order of a few hundreds MeV.

Needless to say that a similar analysis can be performed in any experiment where disappearance and appearance channels are simultaneously available. At the Neutrino Factory, for example (see [17, 18]), the  $\bar{\nu}_\mu$  disappearance channel can be certainly used together with the appearance channel  $\nu_e \rightarrow \nu_\mu$ , whereas the  $\nu_e$  disappearance channel is extremely difficult to exploit (due to the need to measure the electron charge to distinguish  $\nu_e \rightarrow \nu_e$  from  $\bar{\nu}_\mu \rightarrow \bar{\nu}_e$ ).

---

<sup>1</sup>Other  $\beta$ -Beam proposals with different choices of the boosting factor can be found in [12]-[14].

The eightfold degeneracy for these two facilities has been comprehensively studied in [19] and we refer to that paper for all the technical details regarding the used cross-sections, efficiencies and backgrounds. The results of [19] show that to run the two facilities simultaneously does not help in solving the degeneracies, mainly because the two beams, running on the same baseline and with approximately the same energy, are not complementary at all: only the statistics is increased in roughly a factor two, but no *synergy* is achieved (if not for using the same detector, thus halving the corresponding costs). For this reason, in the following we will analyse the performance of the two facilities separately.

## 2 $\beta$ -Beam Appearance and Disappearance Channels

The considered  $\beta$ -Beam setup consists of a  $\bar{\nu}_e$ -beam produced by the decay of  ${}^6\text{He}$  ions boosted at  $\gamma = 60$  and of a  $\nu_e$ -beam produced in the decay of  ${}^{18}\text{Ne}$  ions boosted at  $\gamma = 100$ . The  $\gamma$ -ratio has been chosen to store both ions simultaneously into the decay ring. A flux of  $2.9 \times 10^{18}$   ${}^6\text{He}$  decays/year and  $1.1 \times 10^{18}$   ${}^{18}\text{Ne}$  decays/year, as discussed in [20], will be assumed. The average neutrino energies of the  $\nu_e, \bar{\nu}_e$  beams corresponding to this configuration are 0.37 GeV and 0.23 GeV, respectively. Although the boosting factor has been chosen to maximize the oscillation probability at  $L = 130$  km, a severe drawback of this option is the impossibility to use energy resolution, due to nuclear effects.

	No Osc.	$\theta_{13} = 8^\circ; +$	$\theta_{13} = 8^\circ; -$	$\theta_{13} = 2^\circ; +$	$\theta_{13} = 2^\circ; -$
$N_{e-}$	133205	89426	89742	93837	93865
$N_{e+}$	19557	12180	12158	13000	12999

Table 1: *Disappearance event rates for a 10 years run at the considered  $\beta$ -Beam with a 440 kton detector at  $L = 130$  km, for different values of  $\theta_{13}$  and of the sign of the atmospheric mass difference,  $s_{atm}$ . Appearance event rates have been quoted in ref. [19].*

The measurement of  $(\theta_{13}, \delta)$  at this facility has been already actively discussed in the literature [17, 21]. In particular, a complete analysis of the eightfold degeneracy was done in [19]. In Fig. 1 we plot our results for three different CP phases,  $\bar{\delta} = 0^\circ$  (left plot) and  $\bar{\delta} = 45^\circ, -90^\circ$  (right plot), and for two different mixing angles  $\bar{\theta}_{13} = 2^\circ$  and  $8^\circ$ . The input  $(\bar{\theta}_{13}, \bar{\delta})$  value used in the fit is always shown as a filled black box. As in [19], we use the following reference values for the atmospheric and solar parameters:  $\Delta m_{atm}^2 = 2.5 \times 10^{-3}$  eV<sup>2</sup>,  $\theta_{12} = 33^\circ$  and  $\Delta m_{sol}^2 = 8.2 \times 10^{-5}$  eV<sup>2</sup> [22]. The atmospheric mixing angle,  $\theta_{23}$ , has been fixed at  $\theta_{23} = 40^\circ$ , thus inducing the so-called octant degeneracies<sup>2</sup>. The 90% CL contours for each of the degenerate solutions are depicted in the plot: continuous lines stand for  $s_{atm} = \bar{s}_{atm}, s_{oct} = \bar{s}_{oct}$  (the *true* solution and the *intrinsic* clone); dotted lines stand for  $s_{atm} = -\bar{s}_{atm}, s_{oct} = \bar{s}_{oct}$  (the *sign* clone); dashed lines stand for  $s_{atm} = \bar{s}_{atm}, s_{oct} = -\bar{s}_{oct}$

<sup>2</sup>This will be the case if the T2K experiment observes non-maximal mixing in the atmospheric sector. Notice that a choice of  $\theta_{23} = 50^\circ$  would give similar results.

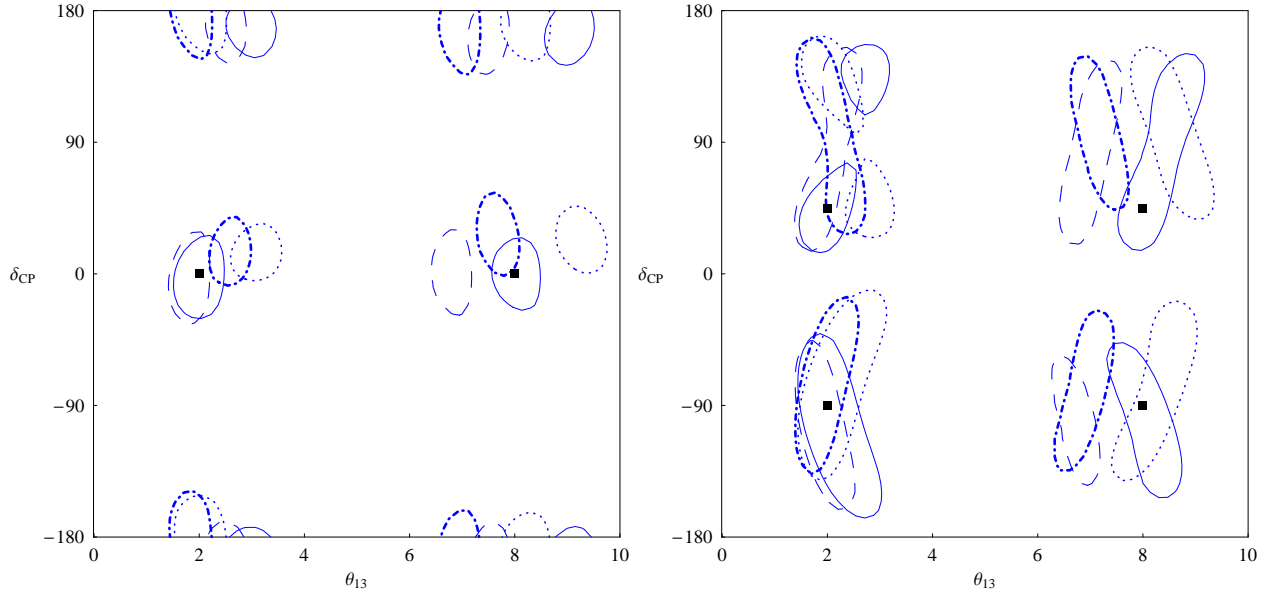


Figure 1: 90% *CL* contours in the  $(\theta_{13}, \delta)$  plane using the appearance channel after a 10 years run at the  $\beta$ -Beam with a 440 kton detector located at  $L = 130$  km, for two different values of  $\theta_{13}$ ,  $\bar{\theta}_{13} = 2^\circ, 8^\circ$ , and three values of  $\delta$ ,  $\bar{\delta} = 0^\circ$  (left plot) and  $\bar{\delta} = 45^\circ, -90^\circ$  (right plot). A 5% systematic error is assumed and backgrounds are computed as in ref. [19]. Continuous, dotted, dashed and dot-dashed lines stand for the intrinsic, sign, octant and mixed degeneracies, respectively.

(the *octant* clone); dot-dashed lines stand for  $s_{atm} = -\bar{s}_{atm}, s_{oct} = -\bar{s}_{oct}$  (the *mixed* clone). These plots are obtained assuming a 5% systematic error. Backgrounds have been computed as in [19].

In Fig. 1 it can be seen the dramatic impact that degeneracies have in the precision of the measure of  $(\theta_{13}, \delta)$ : (1) the error in the  $\theta_{13}$  measurement is increased by a factor four (two) for large<sup>3</sup> (small) values of  $\theta_{13}$ . The presence of degeneracies has a small impact on the ultimate  $\theta_{13}$  sensitivity; (2) the error in the  $\delta$  measurement grows in a significant way in presence of the clones, almost spanning half of the parameter space for small values of  $\theta_{13}$ . These facts are well understood. From the appearance channel of a counting experiment, like the standard  $\beta$ -Beam, with a baseline of hundreds of km there are not enough independent informations to cancel any of the degeneracies.

It has been claimed [25] that the  $\bar{\nu}_e$  disappearance channel at a reactor experiment can help Super-Beam experiments in solving part of the eightfold degeneracy. Indeed, the  $\nu_e$  disappearance probability does not depend on the CP violating phase  $\delta$  and the atmospheric  $\theta_{23}$  mixing angle. Thus, the  $\theta_{13}$  measurement is not affected by  $\theta_{13} - \delta$  correlations nor by the octant and mixed ambiguities. The  $\nu_e \rightarrow \nu_e$  matter oscillation probability, expanded at

<sup>3</sup>The shift in  $\theta_{13}$  of the clones with respect to the true solution is proportional to  $\theta_{13}$ ; see [24] for the explicit derivation.

second order in the small parameters  $\theta_{13}$  and  $(\Delta m_{sol}^2 L/E)$  reads [26]:

$$P_{\mp}(\nu_e \rightarrow \nu_e) = 1 - \left(\frac{\Delta_{atm}}{B_{\mp}}\right)^2 \sin^2 2\theta_{13} \sin^2\left(\frac{B_{\mp}L}{2}\right) - \left(\frac{\Delta_{sol}}{A}\right)^2 \sin^2 2\theta_{12} \sin^2\left(\frac{AL}{2}\right) \quad (2)$$

where  $\Delta_{atm} = \Delta m_{atm}^2/2E$ ,  $\Delta_{sol} = \Delta m_{sol}^2/2E$  and  $B_{\mp} = |A \mp \Delta_{atm}|$  with  $\mp$  for neutrinos (antineutrinos), respectively. The dependence on the sign of the atmospheric mass difference arises from the first non-trivial term of eq. (2) and from higher order terms,  $\mathcal{O}(\theta_{13}^2 \times \Delta m_{12}^2 L/E)$ . As a consequence, the  $s_{atm}$  dependence is relevant for large values of  $\theta_{13}$ , only.

In Tab. 1 we summarize the relevant numbers for the  $\beta$ -Beam disappearance analysis. In the appearance analysis having a realistic description of backgrounds and efficiencies is of fundamental importance for providing the correct sensitivity on  $(\theta_{13}, \delta)$ . Conversely, their relevance is much smaller in the disappearance measure, that is limited primarily by systematic errors. Lacking a complete realistic description of systematics we decided to present in Fig. 2 the disappearance measure for three different systematic errors, namely 0% (“theoretical-unrealistic” scenario), 2% (“optimistic” scenario) and 5% (“pessimistic” scenario). We decided to show the 0% systematic line, as we think it is “theoretically” important to have an idea of the ultimate reach of this experiment. The 2% and 5% lines will cover the optimistic and pessimistic feelings about future experimental improvements in understanding a Mton water detector.

In Fig. 2 the 90% CL contours in the  $(\theta_{13}, \Delta m_{atm}^2)$  plane using the  $\nu_e$  disappearance channel are shown for the input values  $\bar{\theta}_{13} = 2^\circ, 8^\circ$  and  $\Delta m_{atm}^2 = 2.5 \times 10^{-3} \text{ eV}^2$ . The left plot ( $\bar{\theta}_{13} = 2^\circ$ ) represents, in practice, the  $\theta_{13}$  sensitivity reach of the  $\beta$ -Beam disappearance channel. If systematic errors cannot be controlled better than the 5% level, the  $\beta$ -Beam disappearance channel alone does not improve significantly the present bound on  $\theta_{13}$ . The “theoretical” sensitivity (sys=0%) is around  $\theta_{13} = 4^\circ$ , while if a systematics of 2% is achieved the disappearance channel alone could test  $\theta_{13}$  down to  $6^\circ$ . In Fig. 2(right) we show our results for a large value of  $\theta_{13}$ ,  $\bar{\theta}_{13} = 8^\circ$ . With a systematics of 2% the mixing angle can be measured in the disappearance channel alone with an error of  $\pm 2^\circ$ . Again if the 5% systematics is assumed no improvement on the present bound is obtained.

As it is clear from Fig. 2, the  $\nu_e$  disappearance channel is only slightly sensitive to the sign clone, as the full and dashed lines are almost superimposed for every value of  $\theta_{13}$  and  $\Delta m_{atm}^2$ . The  $\nu_e$  disappearance channel is an almost “clone-free” environment for the  $\beta$ -Beam, as it is for reactor experiments. However, even in the case of an optimistic (but non-zero) 2% systematic error, no improvement is obtained adding the disappearance channel informations to the results of Fig. 1 for the appearance channel. The resulting 90% CL contours practically coincide with the previous ones, and for this reason we do not consider to present them in a separate figure. The  $\theta_{13}$  indetermination coming from the clone presence in the appearance channel is smaller than the disappearance error itself. Only considering an unrealistic 0% systematics the disappearance channel starts to be useful to eliminate some of the clones.

Summarizing, the  $\beta$ -Beam has two available oscillation channels: the  $\nu_e \rightarrow \nu_e$  disappearance and the  $\nu_e \rightarrow \nu_\mu$  appearance (and their CP-conjugates). The appearance channel can

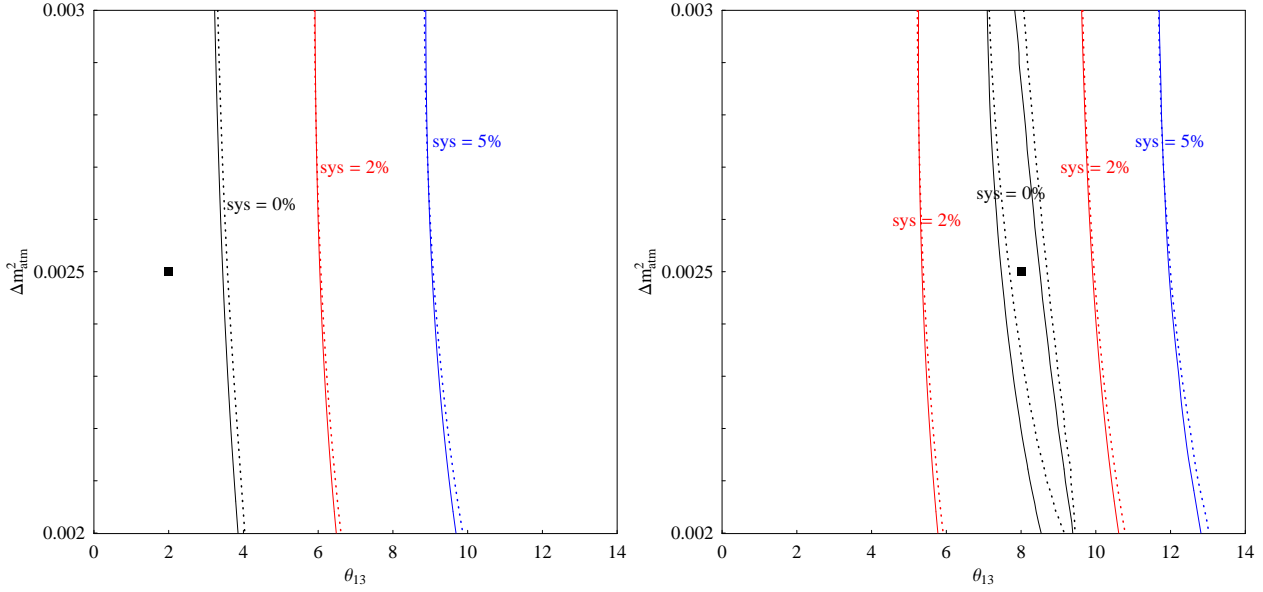


Figure 2: 90% CL contours in the  $(\theta_{13}, \Delta m_{atm}^2)$  plane using the disappearance channel after a 10 years run at the  $\beta$ -Beam for two different values of  $\theta_{13}$ ,  $\bar{\theta}_{13} = 2^\circ$  (left plot) and  $\bar{\theta}_{13} = 8^\circ$  (right plot). Three different values of the systematic errors have been considered: 0% (“theoretical”), 2% (“pessimistic”), 5% (“optimistic”). Continuous lines stand for the true solution, dotted lines stand for the sign degeneracy.

measure  $(\theta_{13}, \delta)$ , but being the considered  $\beta$ -Beam a pure counting experiment this measurement is severely affected by degeneracies. The disappearance channel does not provide any further useful informations once realistic systematic errors are taken into account.

### 3 S-Beam Appearance and Disappearance Channels

The considered Super-Beam setup is a conventional neutrino beam based on the 4 MWatt SPL 2.2 GeV proton driver that has been proposed at CERN, described in ref. [15]. The average neutrino energies of the  $\nu_\mu, \bar{\nu}_\mu$  beams corresponding to this configuration are 0.27 GeV and 0.25 GeV, respectively. The possibility to measure  $(\theta_{13}, \delta)$  with a Super-Beam has been already widely discussed in the literature [27]. A complete analysis of the eightfold degeneracy at this facility has been done in [19].

In Fig. 3 we plot our results for three different CP phases,  $\bar{\delta} = 0^\circ$  (left plot) and  $\bar{\delta} = 45^\circ, -90^\circ$  (right plot), and for two different mixing angles,  $\bar{\theta}_{13} = 2^\circ$  and  $8^\circ$ . The input  $(\bar{\theta}_{13}, \bar{\delta})$  value used in the fit is shown as a filled black box. As in the previous section we use the following reference values for the atmospheric and solar parameters:  $\theta_{23} = 40^\circ$ ,  $\Delta m_{atm}^2 = 2.5 \times 10^{-3} \text{ eV}^2$ ,  $\theta_{12} = 33^\circ$  and  $\Delta m_{sol}^2 = 8.2 \times 10^{-5} \text{ eV}^2$ . The 90% CL contours for each of the degenerate solutions are depicted in the plot and explained in the caption. These plots are obtained assuming a 5% systematic error. Backgrounds have been computed as in [19].

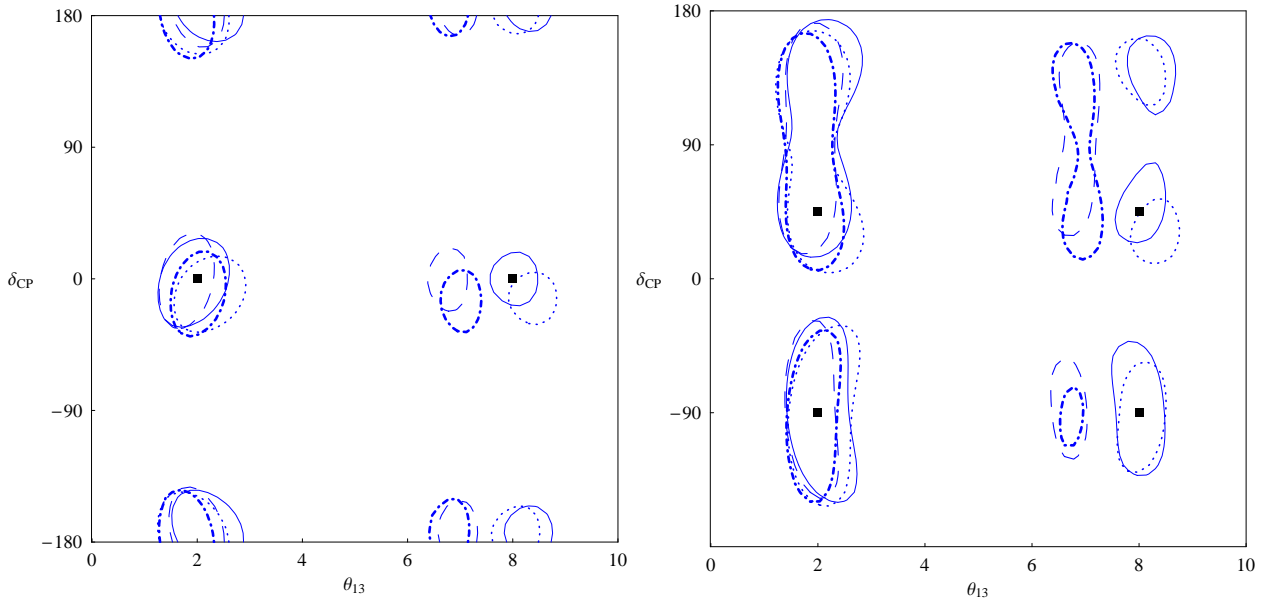


Figure 3: 90% CL contours in the  $(\theta_{13}, \delta)$  plane using the appearance channel after a 2 + 8 years run at the Super-Beam with a 440 kton detector located at  $L = 130$  km, for two different values of  $\theta_{13}$ ,  $\bar{\theta}_{13} = 2^\circ, 8^\circ$ , and three values of  $\delta$ ,  $\bar{\delta} = 0^\circ$  (left plot) and  $\bar{\delta} = 45^\circ, -90^\circ$  (right plot). A 5% systematic error is assumed and backgrounds are computed as in ref. [19]. Continuous, dotted, dashed and dot-dashed lines stand for the intrinsic, sign, octant and mixed degeneracies, respectively.

As it appears from comparison of Fig. 3 with Fig. 1, the “figures of merit” of a standard  $\beta$ -Beam and the SPL Super-Beam are very similar. Also the Super-Beam appearance channel is severely affected by proliferation of clones. The precision in measuring  $(\theta_{13}, \delta)$  is practically identical in the two cases. This is well explained by the comparable statistics in the golden channel ( $\nu_e \rightarrow \nu_\mu$  vs  $\nu_\mu \rightarrow \nu_e$ ) and an almost equal  $(L/E)$  ratio for the two experiments. For this reason there could be no real synergy between this two setups (i.e. they are not complementary) and the only effect in summing these two experiments, concerning the  $(\theta_{13}, \delta)$  measure, is to double the statistics.

Nevertheless, the great advantage of the Super-Beam facility compared with the standard- $\gamma$   $\beta$ -Beam one is the possibility to measure directly the atmospheric parameters using the  $\nu_\mu$  disappearance channel [28] reducing, in particular, the atmospheric mass difference error to less than 10%.

In Tab. 2 we summarize the relevant numbers used in the Super-Beam disappearance analysis. In Fig. 4 we show the measure of  $(\theta_{23}, \Delta m_{atm}^2)$  at the SPL Super-Beam with a 2% systematic error, in the case (left) of non-maximal atmospheric mixing,  $\theta_{23} = 40^\circ$ , and (right) maximal atmospheric mixing,  $\theta_{23} = 45^\circ$ . In both cases, the input value for the atmospheric mass difference has been fixed to  $\Delta m_{atm}^2 = 2.5 \times 10^{-3} \text{ eV}^2$ . The continuous contour represents the fit to the right choice of the sign of the atmospheric mass difference (i.e.  $s_{atm} = \bar{s}_{atm}$ ) whereas the dotted contour represents the fit to the wrong choice of  $s_{atm}$  (i.e.  $s_{atm} = -\bar{s}_{atm}$ ).

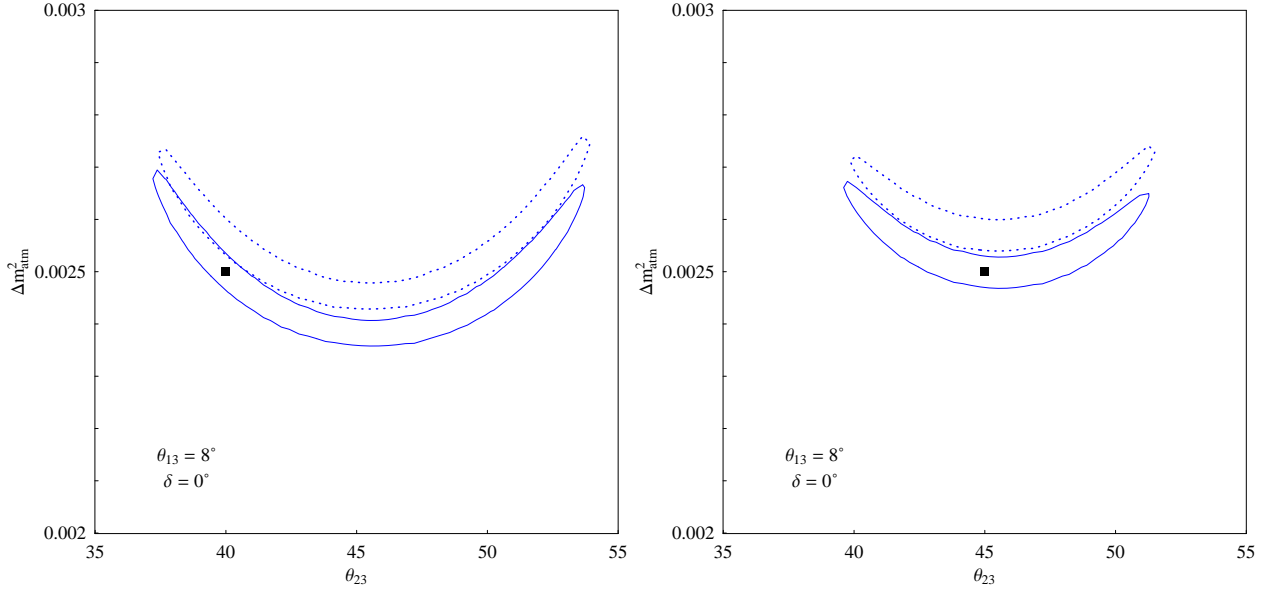


Figure 4: 90% CL contours in the  $(\theta_{23}, \Delta m_{atm}^2)$  plane using the disappearance channel after a 2 + 8 years run at the 4 MWatt SPL Super-Beam for two different values of  $\theta_{23}$ ,  $\theta_{23} = 40^\circ$  (left plot) and  $\theta_{23} = 45^\circ$  (right plot). A systematic error of 2% is assumed. Continuous lines stand for  $s_{atm} = \bar{s}_{atm}$ ; dotted lines stand for  $s_{atm} = -\bar{s}_{atm}$ .

$N_{\mu^-}$	No Osc.	$\theta_{13} = 8^\circ; +$	$\theta_{13} = 8^\circ; -$	$\theta_{13} = 2^\circ; +$	$\theta_{13} = 2^\circ; -$
$\delta = 0^\circ$	24245	2016	2197	1987	2136
$\delta = 90^\circ$		2037	2175	1993	2131
$N_{\mu^+}$	No Osc.	$\theta_{13} = 8^\circ; +$	$\theta_{13} = 8^\circ; -$	$\theta_{13} = 2^\circ; +$	$\theta_{13} = 2^\circ; -$
$\delta = 0^\circ$	25467	1982	2178	1944	2095
$\delta = 90^\circ$		2009	2150	1951	2088

Table 2: Disappearance event rates for a 2 + 8 years run at the 4 MWatt SPL Super-Beam with a 440 kton detector at  $L = 130$  km, for different values of  $\theta_{13}, \delta$  and of the sign of the atmospheric mass difference,  $s_{atm}$ . Appearance event rates have been presented in ref. [19].

Since we plot the results in the full  $\theta_{23} \in [35^\circ - 55^\circ]$  parameter space, the octant and mixed clones in the left plot are automatically taken into account and do not appear as separate regions. Notice, however, that being the contours for  $\theta_{23} \leq 45^\circ$  and  $\theta_{23} \geq 45^\circ$  slightly different for  $\theta_{13} \neq 0^\circ$ , if we were to plot the contours in the  $(\sin^2 2\theta_{23}, \Delta m_{atm}^2)$  plane a fourfold degeneracy would be manifest. In the right plot only the sign clone is present, being  $\theta_{23} = 45^\circ$ . Two comments are in order: first, the sign ambiguity implies that the errors on the atmospheric mass difference are roughly doubled with respect to what expected in the absence of degeneracies; second, the left plot is significantly worse than the right plot. If  $\theta_{23}$

is not maximal, the errors on the atmospheric parameters  $(\theta_{23}, \Delta m_{atm}^2)$  can be much larger than expected.

The presence of degeneracies in the  $\nu_\mu$  disappearance channel can be easily understood looking at the the  $\nu_\mu \rightarrow \nu_\mu$  vacuum oscillation probability expanded to the second order in the small parameters  $\theta_{13}$  and  $(\Delta m_{sol}^2 L/E)$ , [26]:

$$\begin{aligned}
P(\nu_\mu \rightarrow \nu_\mu) &= 1 - (\sin^2 2\theta_{23} - s_{23}^2 \sin^2 2\theta_{13} \cos 2\theta_{23}) \sin^2 \left( \frac{\Delta_{atm} L}{2} \right) \\
&+ \left( \frac{\Delta_{sol} L}{2} \right) \left[ c_{12}^2 \sin^2 2\theta_{23} - \tilde{J} s_{23}^2 \cos \delta \right] \sin(\Delta_{atm} L) \\
&- \left( \frac{\Delta_{sol} L}{2} \right)^2 \left[ c_{23}^4 \sin^2 2\theta_{12} + c_{12}^2 \sin^2 2\theta_{23} \cos(\Delta_{atm} L) \right] \quad (3)
\end{aligned}$$

where  $\tilde{J} = \cos \theta_{13} \sin 2\theta_{12} \sin 2\theta_{13} \sin 2\theta_{23}$ . The first non-trivial term is the dominant (atmospheric) contribution. It does not depend on the solar parameters and it reduces to the usual two-family approximation when  $\theta_{13} = 0^\circ$ . The last term is the subleading solar contribution, suppressed by two powers of the solar mass difference. This term is independent (in this approximation) from  $\theta_{13}$ . Eventually, the term in the second line is the interference between the atmospheric and the solar contributions: it is small but not negligible compared to the first term, being suppressed by only one power of the solar mass difference. This term encodes both a  $\theta_{13}$ -dependence (through the  $\tilde{J}$  coefficient) and a small CP-conserving  $\delta$ -dependence (suppressed by one power of  $\Delta_{sol}$  and one power of  $\theta_{13}$ ). Changing the sign of the atmospheric mass difference makes the interference term change sign, also, mimicking an increase of  $\Delta m_{atm}^2$ . Notice, finally, that the three non-trivial terms in eq. (3) are not symmetric for  $\theta_{23} \rightarrow \pi/2 - \theta_{23}$ . However, the non-symmetric dependence on  $\theta_{23}$  is suppressed by at least two powers of  $\theta_{13}$ ,  $\Delta_{sol}$  or their combination, making the asymmetry extremely small.

In Fig. 5 we present the simultaneous measurement of  $(\theta_{13}, \delta)$  using both the appearance (with a 5% systematic error) and the disappearance (with a 2% systematic error) channels at the Super-Beam. As it can be noticed, contrary to the  $\beta$ -Beam case, the disappearance channel in the Super-Beam fit introduces significant changes. Notably enough, the sign clone has disappeared in any case considered. This is not a surprise as these fits are performed at a fixed  $\Delta m_{atm}^2$ : since in the disappearance channel the sign clone manifests itself at a larger value of  $\Delta m_{atm}^2$  (see Fig. 4), in the combination with the appearance channel the tension between the two suffices to remove the unwanted clone in the  $(\theta_{13}, \delta)$  plane. Notice, moreover, that in some cases the octant clone is considerably reduced or even solved, due to the octant-asymmetric contributions in the disappearance probability, eq. (3). Nonetheless, this does not mean that thanks to the combination of the appearance and the disappearance channels we are indeed able to measure the sign of the atmospheric mass difference,  $s_{atm}$ . The mixed clones are generally still present for large values of  $\theta_{13}$ , thus preventing us from measuring  $s_{atm}$ , if the  $\theta_{23}$ -octant is not known at the time the experiment takes place.

It is clear that these results should be confirmed by a complete multi-dimensional analysis that is actually underway [29]. As a first step, in Fig. 6(left) we show the projection on the  $(\theta_{13}, \delta)$  plane of the Super-Beam appearance three-dimensional fit in the parameters

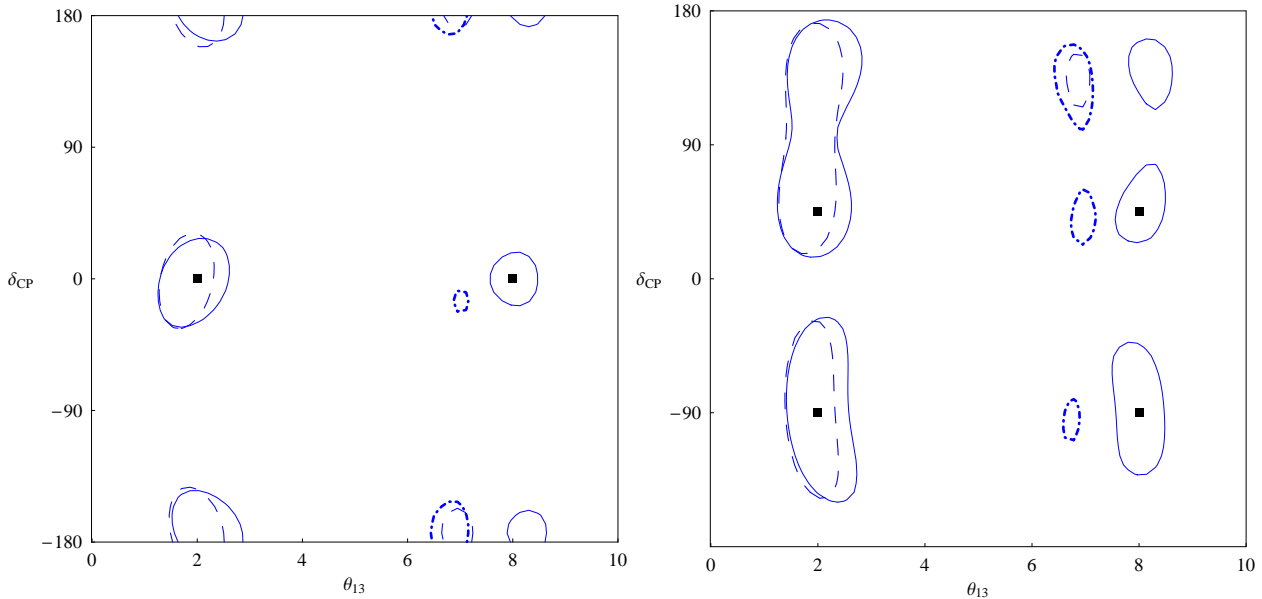


Figure 5: 90% CL contours in the  $(\theta_{13}, \delta)$  plane using the appearance and the disappearance channels after a 2+8 years run at the Super-Beam with a 440 kton detector located at  $L = 130$  km, for two different values of  $\theta_{13}$ ,  $\bar{\theta}_{13} = 2^\circ, 8^\circ$ , and three values of  $\delta$ ,  $\bar{\delta} = 0^\circ$  (left plot) and  $\bar{\delta} = 45^\circ, -90^\circ$  (right plot). A 5% (2%) systematic error is assumed for the appearance (disappearance) channel, and backgrounds are computed as in ref. [19]. Continuous, dotted, dashed and dot-dashed lines stand for the intrinsic, sign, octant and mixed degeneracies, respectively.

$(\theta_{13}, \delta, \Delta m_{atm}^2)$  for the following input values:  $\bar{\theta}_{13} = 8^\circ$ ,  $\bar{\delta} = 45^\circ$  and  $\Delta m_{atm}^2 = 2.5 \times 10^{-3}$  eV<sup>2</sup>. We let  $\Delta m_{atm}^2$  varying freely in the range  $\Delta m_{atm}^2 \in [2.4 - 2.9] \times 10^{-3}$  eV<sup>2</sup>, obtained from Fig. 4. In Fig. 6(right) we show the same three-dimensional fit, adding this time both the Super-Beam appearance and disappearance channels. It can be seen that in a complete three-parameters analysis small remnants of the sign clones are still present, contrary to the case of the two-parameters analysis of Fig. 5. It is, however, still true that the degeneracy structure gets strongly reduced. This represents an enormous advantage compared with the  $\beta$ -Beam option. We stress again that this result strongly relies on using at the same time appearance and disappearance  $\chi^2$ s and cannot be obtained only restricting the allowed range for  $\Delta m_{atm}^2$  to the measured one.

## 4 Sensitivity to $(\theta_{13}, \delta)$

Eventually, in Fig. 7 we present the sensitivity to  $(\theta_{13}, \delta)$  using the appearance channel only or the combination of the appearance and the disappearance channels, for the  $\beta$ -Beam (left) and the Super-Beam (right). The  $3\sigma$  sensitivity contours have been computed as follows: at a fixed  $\bar{\theta}_{13}$ , we look for the smallest (largest) value of  $|\bar{\delta}|$  for which the two-parameters

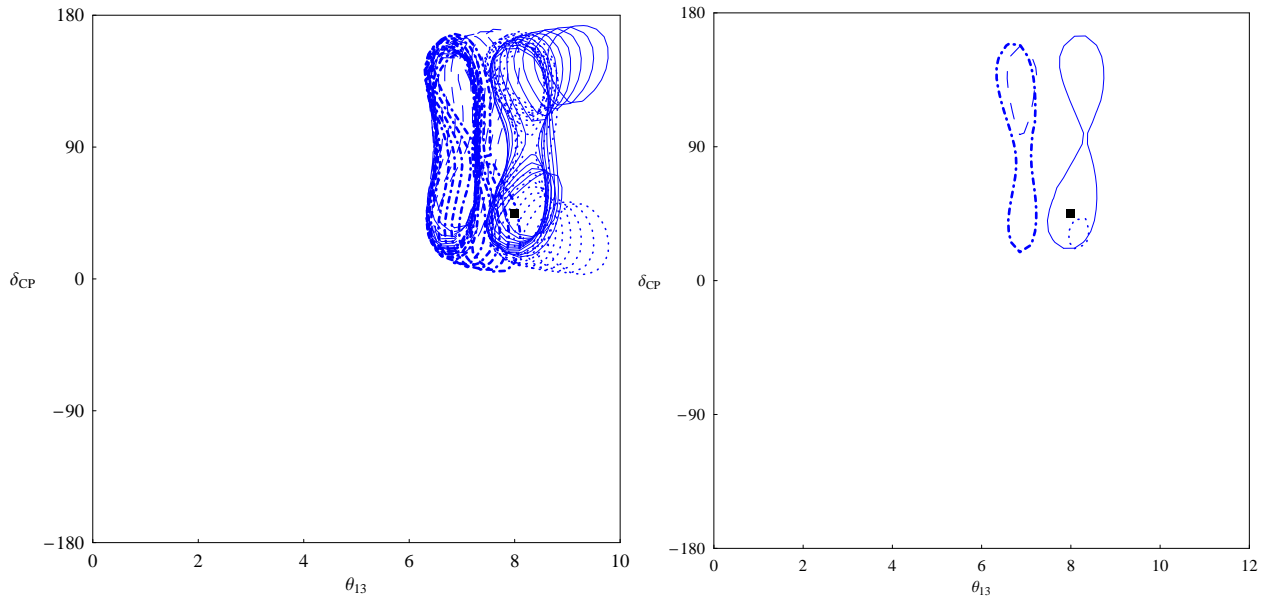


Figure 6: *Projection on the  $(\theta_{13}, \delta)$  plane of the 90% CL three-dimensional contours for the Super-Beam appearance (left) and appearance plus disappearance (right) channels. The fit has been performed in  $(\theta_{13}, \delta, \Delta m_{atm}^2)$  with input values  $\bar{\theta}_{13} = 8^\circ$ ,  $\bar{\delta} = 45^\circ$  and  $\Delta m_{atm}^2 = 2.5 \times 10^{-3} eV^2$ , for  $\theta_{23} = 40^\circ$ .*

$3\sigma$  contours of any of the degenerate solutions (true, sign, octant and mixed) do not touch  $\delta = 0^\circ$  nor  $\delta = 180^\circ$ . Notice that, although the input  $\bar{\theta}_{13}$  value is fixed, the clones can touch  $\delta = 0^\circ, 180^\circ$  at  $\theta_{13} \neq \bar{\theta}_{13}$ , also<sup>4</sup>. The outcome of this procedure is finally plotted, representing the region in the  $(\theta_{13}, \delta)$ -parameter space for which a CP-violating signal is observed at  $3\sigma$ . The novelty of this plot, with respect to Fig. 6 of [20] and to Fig. 13 of [13], is that we fully take into account the impact of the parameter degeneracies to derive the CP-violation discovery power of these facilities. Moreover, we present the results for the whole allowed range in  $\delta$ ,  $\delta \in [-180^\circ, 180^\circ]$ . This is particularly appropriate, since only an approximate symmetry is observed for  $|\delta| \geq \pi/2$  and  $|\delta| \leq \pi/2$  and no symmetry at all between positive and negative  $\delta$ . For both facilities, we have applied a 2% systematic error on the disappearance channel (i.e.,  $\nu_\mu \rightarrow \nu_\mu$  and  $\nu_e \rightarrow \nu_e$ ) and a 5% systematic error on the appearance channel (i.e.,  $\nu_e \rightarrow \nu_\mu$  and  $\nu_\mu \rightarrow \nu_e$ ).

First of all, notice that the Super-Beam sensitivity in  $\theta_{13}$  is symmetric in  $\delta$  (for both sectors, we observe an ultimate sensitivity of  $\sin^2 \theta_{13} \simeq 6 - 8 \times 10^{-4}$ ). This is not the case for the  $\beta$ -Beam, where for positive  $\delta$  the facility outperforms the Super-Beam and for negative  $\delta$  is outperformed by it. We know, however, that this asymmetric behaviour of the  $\beta$ -Beam for positive and negative  $\delta$  is a statistical mirage caused by the low background in

<sup>4</sup>This is not the case of Fig. 11 in ref. [19], where the excluded region in  $\delta$  at fixed  $\bar{\theta}_{13}$  in the absence of a CP-violating signal at 90% CL is presented. In practice, in that figure we compare  $N_\pm(\bar{\theta}_{13}, \delta)$  with  $N_\pm(\bar{\theta}_{13}, 0^\circ)$ , thus obtaining a one-parameter sensitivity plot in  $\delta$  only.

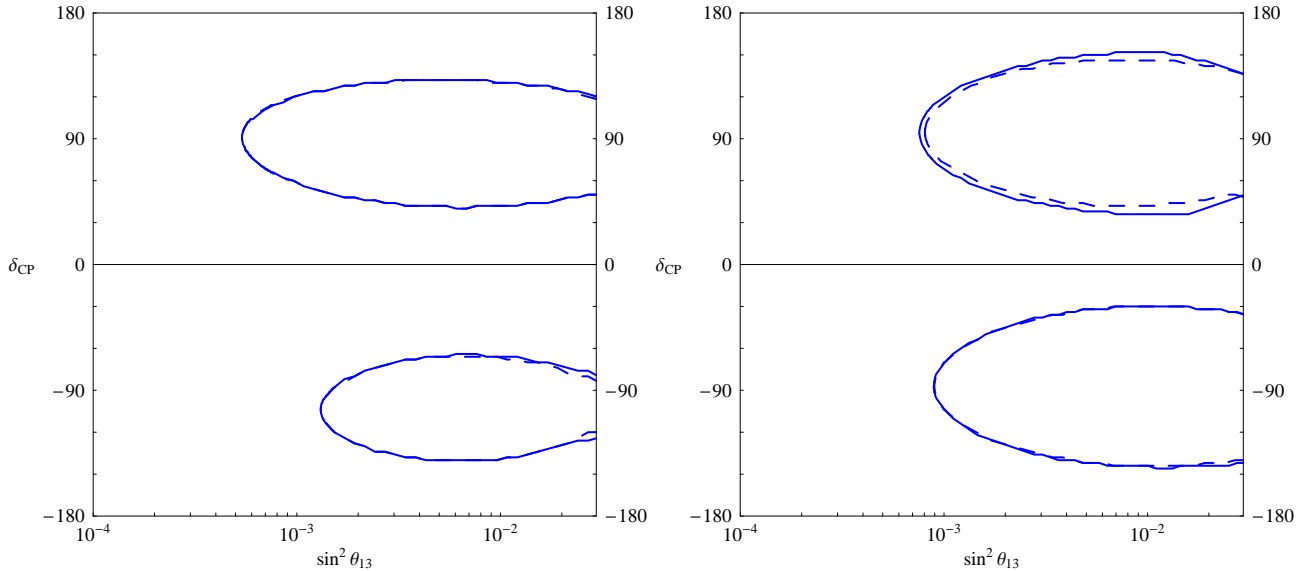


Figure 7:  $3\sigma$  sensitivity plot in the  $(\theta_{13}, \delta)$  plane for the considered  $\beta$ -Beam (left) and Super-Beam (right). Dashed lines stand for appearance channel only, whereas solid lines stand for the combination of the appearance and the disappearance channels at the same facility. A 2% systematic error in the disappearance channel and a 5% systematic error in the appearance channel have been considered for both facilities.

the appearance antineutrino sample and the high background in the appearance neutrino one (see [19]). A proper statistical treatment should be performed, following [30], to get rid of this asymmetry in the small  $\sin^2 \theta_{13}$  case: the treatment, however, is extremely time consuming and we do not consider meaningful applying it here. Regarding the sensitivity to  $\delta$ , notice how for large  $\theta_{13}$  the Super-Beam is generally performing better than the  $\beta$ -Beam, in particular for negative  $\delta$ . This can be understood comparing the right plots in Fig. 1 and Fig. 5: for  $\bar{\theta}_{13} = 8^\circ, \bar{\delta} = -90^\circ$  we can see that the 90% CL contours for the Super-Beam are much smaller than for the  $\beta$ -Beam. For positive  $\delta$  the difference is not so relevant, since although the Super-Beam contours for  $\bar{\theta}_{13} = 8^\circ, \bar{\delta} = 45^\circ$  are certainly smaller than the  $\beta$ -Beam ones, it can be seen that the spread in  $\delta$  is similar.

Eventually, we stress that for the Super-Beam a small improvement in the sensitivity in  $\delta$  is achieved combining appearance and disappearance channels. On the contrary, practically no effect is observed in the  $\beta$ -Beam case.

## 5 Conclusions

Summarizing, in this letter we have tried to understand the impact of a disappearance measurement on the  $(\theta_{13}, \delta)$  eightfold degeneracy for two specific facilities, the 4 MWatt SPL

Super-Beam and the standard low- $\gamma$   $\beta$ -Beam proposed at CERN. We presented a complete analysis of degenerations in the  $\nu_e$  and  $\nu_\mu$  disappearance channels: the  $\nu_e$  disappearance is affected by a twofold degeneracy, since the  $\nu_e$  probability depends on  $s_{atm}$  only, eq. (2); the  $\nu_\mu$  disappearance is affected by a fourfold degeneracy, depending on both  $s_{atm}$  and  $s_{oct}$ , eq. (3).

The standard low- $\gamma$   $\beta$ -Beam setup looks somewhat limited, when compared with facilities with many channels to exploit, such as the Neutrino Factory: indeed, the *golden*  $\nu_e \rightarrow \nu_\mu$  appearance channel is severely affected by degeneracies (being the neutrino energy too low to use energy resolution techniques) and the combination with the  $\nu_e \rightarrow \nu_e$  disappearance, potentially of interest, is in practice useless once a realistic systematic error is taken into account. The  $\beta$ -Beam idea should be certainly pursued further, using for example higher  $\gamma$  options. For neutrino energies around 1 GeV is, in fact, possible to take advantage of energy resolution [31] and, for energies higher than 4-5 GeV, the silver channel  $\nu_e \rightarrow \nu_\tau$  becomes available. In both cases, the different informations can be used to reduce the parameter space degeneracies and solve some of the clones, consequently improving our knowledge on  $\theta_{13}$  and  $\delta$  beyond the Super-Beam reach.

The SPL Super-Beam appearance channel,  $\nu_\mu \rightarrow \nu_e$ , is also severely affected by degeneracies (being a counting experiment, as the  $\beta$ -Beam). However, in this case the complementarity between the appearance and disappearance channels,  $\nu_\mu \rightarrow \nu_e$  and  $\nu_\mu \rightarrow \nu_\mu$ , can be fully exploited even when a realistic systematic error is taken into account. In particular, the sign ambiguity can be strongly reduced (Fig. 6), a consequence of the fact that the disappearance sign clone is located at a different  $\Delta m_{atm}^2$  for different choices of  $s_{atm}$ , Fig. 4. Notice, finally, that the  $\nu_\mu$  disappearance channel is interesting on its own for a precise measurement of the atmospheric oscillation parameters,  $(\theta_{23}, \Delta m_{atm}^2)$ , Fig. 4.

It is clear that, in the case where only one of the two facilities were to be built, the 4 MWatt SPL Super-Beam would represent a more interesting choice than the standard low- $\gamma$   $\beta$ -Beam to study the leptonic mixing matrix. Different  $\beta$ -Beam setups should instead be considered.

## Acknowledgments

We would like to thank B. Gavela, J. Gomez-Cadenas, P. Hernandez, D. Meloni and P. Migliozzi for useful discussions. The authors acknowledge the financial support of MCYT through project FPA2003-04597 and of the European Union through the networking activity BENE.

## References

- [1] Y. Fukuda *et al.* [Super-Kamiokande Collaboration], Phys. Rev. Lett. **81** (1998) 1562 [arXiv:hep-ex/9807003]; M. Ambrosio *et al.* [MACRO Collaboration], Phys. Lett. B **517** (2001) 59 [arXiv:hep-ex/0106049]; M. H. Ahn *et al.* [K2K Collaboration], Phys. Rev. Lett. **90** (2003) 041801 [arXiv:hep-ex/0212007]; B. T. Cleveland *et al.*, Astrophys. J. **496** (1998) 505; J. N. Abdurashitov *et al.* [SAGE Collaboration], Phys. Rev. C **60**

- (1999) 055801 [arXiv:astro-ph/9907113]; W. Hampel *et al.* [GALLEX Collaboration], Phys. Lett. B **447** (1999) 127; S. Fukuda *et al.* [Super-Kamiokande Collaboration], Phys. Rev. Lett. **86** (2001) 5651 [arXiv:hep-ex/0103032]; Q. R. Ahmad *et al.* [SNO Collaboration], Phys. Rev. Lett. **87** (2001) 071301 [arXiv:nucl-ex/0106015]; K. Eguchi *et al.* [KamLAND Collaboration], Phys. Rev. Lett. **90** (2003) 021802 [arXiv:hep-ex/0212021].
- [2] B. Pontecorvo, Sov. Phys. JETP **6** (1957) 429 [Zh. Eksp. Teor. Fiz. **33** (1957) 549]; Z. Maki, M. Nakagawa and S. Sakata, Prog. Theor. Phys. **28** (1962) 870; B. Pontecorvo, Sov. Phys. JETP **26** (1968) 984 [Zh. Eksp. Teor. Fiz. **53** (1967) 1717]; V. N. Gribov and B. Pontecorvo, Phys. Lett. B **28** (1969) 493.
- [3] M. Apollonio *et al.* [CHOOZ Collaboration], Phys. Lett. B **466** (1999) 415 [arXiv:hep-ex/9907037]; M. Apollonio *et al.* [CHOOZ Collaboration], Eur. Phys. J. C **27** (2003) 331 [arXiv:hep-ex/0301017].
- [4] A. Cervera *et al.*, Nucl. Phys. B **579** (2000) 17 [Erratum-ibid. B **593** (2001) 731] [arXiv:hep-ph/0002108].
- [5] J. Burguet-Castell *et al.*, Nucl. Phys. B **608** (2001) 301 [arXiv:hep-ph/0103258].
- [6] H. Minakata and H. Nunokawa, JHEP **0110** (2001) 001 [arXiv:hep-ph/0108085].
- [7] G. L. Fogli and E. Lisi, Phys. Rev. D **54** (1996) 3667 [arXiv:hep-ph/9604415].
- [8] V. Barger, D. Marfatia and K. Whisnant, Phys. Rev. D **65** (2002) 073023 [arXiv:hep-ph/0112119].
- [9] H. Minakata, H. Nunokawa and S. J. Parke, Phys. Rev. D **68** (2003) 013010 [arXiv:hep-ph/0301210]; O. Yasuda, arXiv:hep-ph/0405005.
- [10] A. Donini, D. Meloni and P. Migliozzi, Nucl. Phys. B **646** (2002) 321 [arXiv:hep-ph/0206034]; D. Autiero *et al.*, Eur. Phys. J. C **33** (2004) 243 [arXiv:hep-ph/0305185].
- [11] P. Zucchelli, Phys. Lett. B **532** (2002) 166.
- [12] C. Volpe, J. Phys. G **30** (2004) L1 [arXiv:hep-ph/0303222].
- [13] J. Burguet-Castell *et al.*, arXiv:hep-ph/0312068.
- [14] F. Terranova *et al.*, arXiv:hep-ph/0405081.
- [15] J. J. Gomez-Cadenas *et al.* [CERN working group on Super Beams Collaboration], arXiv:hep-ph/0105297.
- [16] C. K. Jung, arXiv:hep-ex/0005046.
- [17] C. Albright *et al.*, arXiv:hep-ex/0008064; M. Apollonio *et al.*, arXiv:hep-ph/0210192.

- [18] A. Blondel *et al.*, Nucl. Instrum. Meth. A **451** (2000) 102.
- [19] A. Donini *et al.*, arXiv:hep-ph/0406132.
- [20] J. Bouchez, M. Lindroos and M. Mezzetto, arXiv:hep-ex/0310059.
- [21] M. Mezzetto, J. Phys. G **29** (2003) 1771 [arXiv:hep-ex/0302007]; A. Blondel *et al.*, CERN-2004-002; M. Mezzetto, arXiv:hep-ex/0410083.
- [22] S. Goswami, A. Bandyopadhyay and S. Choubey, arXiv:hep-ph/0409224;
- [23] M. C. Gonzalez-Garcia, arXiv:hep-ph/0410030.
- [24] A. Donini, D. Meloni and S. Rigolin, JHEP **0406**, 011 (2004) [arXiv:hep-ph/0312072].
- [25] H. Minakata *et al.*, Phys. Rev. D **68** (2003) 033017 [arXiv:hep-ph/0211111]; H. Minakata and H. Sugiyama, Phys. Lett. B **580** (2004) 216 [arXiv:hep-ph/0309323]; K. Anderson *et al.*, arXiv:hep-ex/0402041; H. Sugiyama *et al.*, arXiv:hep-ph/0409109.
- [26] E. K. Akhmedov *et al.*, JHEP **0404** (2004) 078 [arXiv:hep-ph/0402175].
- [27] H. Minakata and H. Nunokawa, Phys. Lett. B **495** (2000) 369 [arXiv:hep-ph/0004114]; V. D. Barger *et al.*, Phys. Rev. D **63** (2001) 113011 [arXiv:hep-ph/0012017]; V. D. Barger *et al.*, arXiv:hep-ph/0103052; H. Minakata and H. Nunokawa, JHEP **0110** (2001) 001 [arXiv:hep-ph/0108085]; P. Huber, M. Lindner and W. Winter, Nucl. Phys. B **645** (2002) 3 [arXiv:hep-ph/0204352]; G. Barenboim *et al.*, arXiv:hep-ex/0206025; J. E. Campagne and A. Cazes, arXiv:hep-ex/0411062.
- [28] H. Minakata, M. Sonoyama and H. Sugiyama, arXiv:hep-ph/0406073.
- [29] A. Donini *et al.*, work in preparation.
- [30] G. J. Feldman and R. D. Cousins, Phys. Rev. D **57** (1998) 3873.
- [31] Y. Itow *et al.*, arXiv:hep-ex/0106019.